

# Modeling the Point-to-Point Wireless Communication Channel under the Adverse Weather Conditions

Sermsak JARUWATANADILOK<sup>†a)</sup>, Urachada KETPROM<sup>†</sup>, Yasuo KUGA<sup>†</sup>, *Nonmembers,*  
and Akira ISHIMARU<sup>†</sup>, *Member*

**SUMMARY** Point-to-point optical and millimeter wave communication has recently been of interest, especially in urban areas. Its benefits include simpler and easier installation compared with a land-based line. However, this technology suffers when adverse weather conditions are present, such as rain, fog and clouds, which induce scattering and absorption of the optical wave. The effects of scattering and absorption degrade the quality of the communication link resulting in increase of bit-error-rate. Therefore, there exists a need for accurate channel characterization in order to understand and mitigate the problem. In this paper, radiative transfer theory is employed to study the behavior of amplitude modulated signal propagating through a random medium. We show the effect of the medium to a modulated signal and relate the outcome on the quality of the communication link.

**Key words:** multiple scattering, radiative transfer theory, random media, optical wave propagation, free space optics, millimeter-wave

## 1. Introduction

Point-to-point optical (free space optics or FSO) and millimeter-wave (MMW) communication has been of interest in recent years due to the increase in demand for high-speed data links, especially in urban areas. FSO and MMW links provide simple and fast installation. Both systems require a line-of-sight propagation channel and are affected by adverse weather conditions such as fog, clouds, and rain. The maximum data rate is often limited by the channel condition. Therefore, an accurate model of the communication channel is required in order to characterize and improve the quality of the communication link.

The deterioration of the propagation channel can be classified into two cases: (i) due to fluctuation of index of refraction and (ii) due to volume scattering by atmospheric particulates. For a short distance communication link, the dominant effect usually comes from the volume scattering and we will focus on it in this paper. This is particularly true for the MMW link.

When the size parameter  $ka$ , where  $k$  is the wave number and  $a$  is a radius of the particle, is much smaller than 1, the scattering is almost isotropic, and we can apply the Rayleigh approximation. On the other hand, when  $ka$  is greater than 1 which happens when the particle size becomes comparable to the wavelength, the Mie scattering solution should be used [1]. FSO communication operates in

the optical frequency range, and the common wavelengths are around  $0.85\ \mu\text{m}$  and  $1.5\ \mu\text{m}$ . Therefore, fog and clouds which have particle sizes in the same range have a strong effect on FSO. However, for the MMW system with a wavelength of few millimeters, rain will be the major problem. In both cases, scattering and absorption of the wave by discrete particles results in deterioration of the communication link.

One of the most accurate ways to characterize wave propagation through random media is the exact numerical solution for the radiative transfer theory. Although the radiative transfer theory is based on the conservation of energy and is less strict than the solutions of the fundamental Maxwell's equation, we are only interested in the modulated intensity (or power), and the full wave solution which is very difficult to obtain is not required in our case. The ON-OFF keying imposed on a carrier frequency, such as a digitally modulated optical beam, can be viewed as an amplitude modulation on carrier frequency. Because the square wave can be decomposed into Fourier components, if we solve the radiative transfer equation for different modulation frequencies and combine all the frequency responses, we should be able to simulate the ON-OFF keying modulation. The fundamental radiative transfer equation is modified to include the frequency modulation, which we explained in details in our previous papers [2], [3]. The frequency modulated wave or photon density wave has been used in several applications because it is believed to better sustain the scattering effect in turbid media [4], [5].

In this paper, we explain the limitation and the justification of using the radiative transfer theory for FSO and MMW communication channels. Then, we express the vector radiative transfer equation with frequency modulation and obtain its solution. The numerical results for different cases will be discussed.

## 2. Channel Characterization Using Radiative Transfer Theory

In classical communication theory, the channel can be characterized in the time domain or in the frequency domain. In the time domain, the impulse response exhibits the time characteristic of the channel. On the other hand, in the frequency domain, the frequency response which is the Fourier transform of the impulse response, shows the characteristics of the channel as a function of frequency. For a frequency limited signal, the frequency response is a more compact

Manuscript received January 20, 2004.

Manuscript revised March 11, 2004.

<sup>†</sup>The authors are with the Department of Electrical Engineering, University of Washington, Seattle, WA 98195, USA.

a) E-mail: sermsak@ee.washington.edu

way to evaluate the channel characteristics. We want to investigate the response to an information carrying optical wave. In this investigation, we consider the ON-OFF keying modulation. We assume that the data transmitted through the channel is a square wave which represents alternating zero digits and one digits. The frequency spectrum of the input wave is easily realized as a Fourier series with a fundamental frequency of half of the bit rate. Frequency components of the input pulse is an infinite series of odd harmonics of the fundamental frequency. However, at higher harmonics the amplitude is reduced by a factor  $1/N$  where  $N$  is the harmonic order. Therefore, we can ignore the contribution from a higher order. As a result, characterizing of the channel using the ON-OFF keying signal in the frequency domain will reduce the computational resource required and provide adequate information.

To characterize the propagation channel, the scattering and absorption effect from the medium have to be accounted for. One way is to start with analytical theory involving Maxwell's equations. This method is complete in the sense that all wave phenomena are included, but it poses a mathematical challenge and, in practice, is nearly impossible to solved [6]. The radiative transfer equation, on the other hand, starts with statement of energy conservation. Thus, it relaxes the rigorous mathematics which exists in Maxwell's equations. However, it does not include some of the wave phenomenon. It also assumes there is no correlation between fields. In this particular problem where only the intensity is of consideration, radiative transfer theory can be applied to explain the behavior of the intensity of the wave propagating through a random scattering medium.

We model both the FSO and MMW channels with the following assumptions. The medium is a slab of a homogeneous background of air with suspended particles. The particles are assumed to be spherical water droplets. The distribution of the particles throughout the slab is uniform. An important parameter indicating the randomness of the medium is the optical depth  $\tau_o$  defined by  $\tau_o = \rho\sigma_t L$  where  $L$  is the length of medium. In our calculation, we use  $L = 200$  m. The concentration of particles  $\rho$  depends on the condition of the weather. This parameter should be carefully considered since radiative transfer theory works only in the case where the particles are not too dense. The total scattering cross section of a single particle  $\sigma_t$  can be calculated using the Mie solution with assumption of spherical shape.

In the FSO channel, we employ data from reference [7] which give the distribution of fog particles in Table 1. The wavelength used in the calculation is 0.8 micron. We consider cases of weather varying from light fog with visibility about 1–5 km corresponding to optical depth of about 0.8 to the heavy fog with visibility less than 200 m corresponding to the optical depth of more than 7 [8]. Our calculations show the result of the optical depth of 1 and 15. For the MMW case, we use a frequency of 220 GHz and the particle distribution of rain given by reference [9]. We consider four types of rain ranging from light rain (1 mm/hr) to heavy

**Table 1** Particle size distribution of fog.

Diameter of Particle ( $\mu\text{m}$ )	Number of particles
0.4	3
0.6	10
0.7	40
1.4	50
2.0	7
3.6	1
5.4	9
8.0	2

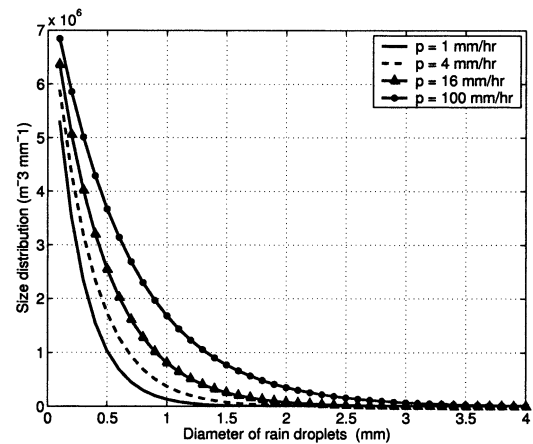


**Fig. 1** Size distribution of rain droplets.

rain (100 mm/hr). Figure 1 shows the volume distribution for several rain rates.

The signal is an ON-OFF keying modulation with a modulation frequency of 50 MHz and 500 MHz corresponding to the bit rate of 100 Mbit/sec and 1 Gbit/sec. The ON-OFF keying signal can be decomposed in the Fourier series with odd harmonics with respect to the fundamental frequency. We are able to calculate the intensity of the wave at particular frequencies using the radiative transfer and recombine them to construct the response of the input optical wave. As Fig. 2 shows, the FSO signal consists of the DC term and the AC term. Both have to be considered to complete the reconstruction of the output signal. Each term creates the coherent and incoherent contribution to the signal after propagation through the medium. Therefore, there are four terms that contribute to the output signal. Coherent components are the result of waves that are not affected by scattering and absorption. The amplitude of this component dramatically drops as a function of the optical length  $\rho\sigma_t z$  where  $z$  is the distance in meters. As a result, at the other end of the medium ( $z = L$ ), the reduction is  $\exp(-\tau_o)$ . On the other hand, the incoherent components encounter multiple scattering. These components obey the radiative transfer theory. To find the output intensity on these components, the radiative transfer equation must be employed. We choose the frequency-domain pulse-vector radiative transfer equation which is an extension of the well-known radiative trans-

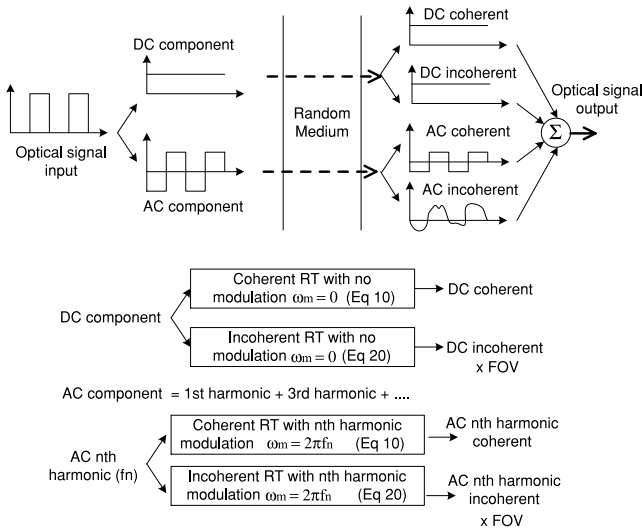


**Fig. 2** Model of optical propagation through a random medium using radiative transfer theory.

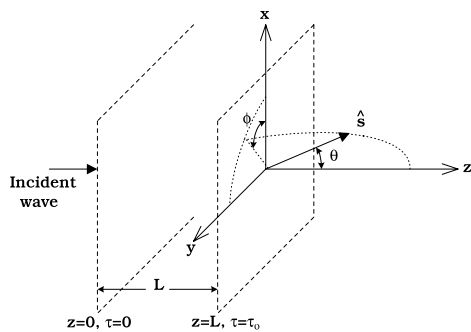


**Fig. 3** Plane parallel problem.

fer equation [10]. The frequency domain gives the capability to solve for a modulated signal. The vector formulation provides information about the polarization. Thus, we can find solution in any kind of polarization orientation, circular or linear. Solving the incoherent component of the DC term is merely solving the radiative transfer equation with no modulation. However, the incoherent component of the AC term is the solution of the radiative transfer equation with frequency modulation. With the Fourier series expansion, we can solve each harmonic separately.

There is an important parameter for the receiver called field-of-view (FOV) which is the indication of ability to capture the intensity [11]. Wide FOV receivers are able to capture more intensity which improves the signal-to-noise ratio, but also increases the effect from scattering because they also capture multiple scattered signals.

The limitation and justification of this modelling are the following. Based on radiative transfer, the medium cannot be too dense. We limit ourselves to the plane wave incidence on a plane parallel geometry shown in Fig. 3 because the formulation and computations can be simplified substantially. This approximation of plane wave should be valid in this case since the geometry in these calculation can

be considered in the far-field regime. This geometry is also a reasonable assumption in practice. In general, radiative transfer theory should work in any geometry with careful consideration of the boundary conditions. We assume that the particle is spherical to be able to use the well-established Mie solution to calculate the phase function. Any other particle shapes can be included if their phase functions can be calculated.

### 3. Radiative Transfer Equation and Its Solutions

The frequency-domain pulse-vector radiative transfer equation in plane-parallel problem is given by

$$\begin{aligned} & \left( \mu \frac{\partial}{\partial \tau} + 1 - i \frac{\omega}{\tau_o} \right) \mathbf{I}(\omega, \tau, \mu, \phi) \\ & = \int_0^{2\pi} \int_{-1}^1 \mathbf{S}(\mu, \phi, \mu', \phi') \mathbf{I}(\omega, \tau, \mu', \phi') d\mu' d\phi' \\ & + \mathbf{J}(\omega, \tau, \mu, \phi), \text{ for } 0 \leq \tau \leq \tau_o \end{aligned} \quad (1)$$

where  $\mathbf{I}$  is the modified Stokes parameter given by

$$\mathbf{I} = \begin{bmatrix} I_1 & I_2 & U & V \end{bmatrix}^T = \begin{bmatrix} \langle E_1 E_1^* \rangle & \langle E_2 E_2^* \rangle \\ 2\Re \langle E_1 E_2^* \rangle & 2\Im \langle E_1 E_2^* \rangle \end{bmatrix}^T \quad (2)$$

$\mu = \cos(\theta)$ . The optical distance  $\tau$  is given by  $\tau = \rho \sigma_t z$ .  $\mathbf{S}$  is the scattering matrix or Mueller matrix given by

$$\mathbf{S} = \begin{bmatrix} S_1 & S_2 \\ S_3 & S_4 \end{bmatrix} \quad (3)$$

where submatrices  $S_1, S_2, S_3, S_4$  are given by

$$S_1 = \begin{bmatrix} |f_{11}|^2 & |f_{12}|^2 \\ |f_{21}|^2 & |f_{22}|^2 \end{bmatrix} \quad (4)$$

$$S_2 = \begin{bmatrix} \Re(f_{11}f_{12}^*) & -\Im(f_{11}f_{12}^*) \\ \Re(f_{21}f_{22}^*) & -\Im(f_{21}f_{22}^*) \end{bmatrix} \quad (5)$$

$$S_3 = \begin{bmatrix} 2\Re(f_{11}f_{21}^*) & 2\Re(f_{12}f_{22}^*) \\ 2\Im(f_{11}f_{21}^*) & 2\Im(f_{12}f_{22}^*) \end{bmatrix} \quad (6)$$

$$S_4 = \begin{bmatrix} 2\Re(f_{11}f_{22}^* + f_{12}f_{21}^*) & -2\Im(f_{11}f_{22}^* - f_{12}f_{21}^*) \\ 2\Im(f_{11}f_{22}^* + f_{12}f_{21}^*) & -2\Re(f_{11}f_{22}^* - f_{12}f_{21}^*) \end{bmatrix} \quad (7)$$

The scattering amplitudes  $f_{11}, f_{12}, f_{21}$ , and  $f_{22}$  are given by Cheung and Ishimaru [12].  $\mathbf{J}$  is the source term. In most cases, the particles have various sizes, which may be expressed in a size distribution. We calculate the scattering amplitude at all size and then use the distribution of the size to make an average. Thus, the resultant scattering amplitudes capture the characteristics of all the particle in an average fashion.

The input signal is the combination of the DC term and the AC term expressed as

$$\mathbf{I}_{total}(t) = \mathbf{I}_{DC} + \mathbf{I}_{AC}(t) \exp(i\omega_{mod}t) \quad (8)$$

where  $\omega_{mod} = 2\pi f_{mod}$  and  $f_{mod}$  is the modulation frequency. The derivation from now on is based on the AC term which

includes the modulation. The derivation and solution of the DC term is the same except that the modulation frequency is set to zero.

The solution of the radiative transfer equation can be separated into reduced (coherent) intensity and diffuse (incoherent) intensity. Reduced intensity is the component that does not encounter the multiple scattering from the medium. Thus, the contribution from the scattering matrix **S** is ignored. It obeys the equation

$$\frac{\partial}{\partial \tau} \mathbf{I}_{ri} = -\mathbf{I}_{ri} \quad (9)$$

The solution to this equation in the normally incident plane wave case is

$$\mathbf{I}_{ri}(t, \tau) = \mathbf{I}_o f(t, \tau) \exp(-\tau) \delta(\phi) \delta(\mu - 1) \quad (10)$$

where  $\mathbf{I}_o$  is the incident modified Stokes vector. The pulse shape function  $f(t, \tau)$  for continuous wave is defined by

$$f(t, \tau) = \exp\left[-i\omega_m \left(t - \frac{\tau}{\tau_o}\right)\right] \quad (11)$$

where  $\omega_m = \omega_{mod}(L/c)$  is the normalized angular modulation frequency. Note that  $t$  in this equation is also the normalized time ( $t_n = t(c/L)$ ) but, throughout this paper, we omit the subscript 'n'.

To find the solution to the diffuse component, we go back to the frequency dependent equation (Eq. (1)) where the source term is the result of the incident modified vector. The diffused modified Stokes vector  $\mathbf{I}_d$  satisfies

$$\begin{aligned} & \left(\mu \frac{\partial}{\partial \tau} + 1 - i \frac{\omega}{\tau_o}\right) \mathbf{I}_d(\omega, \tau, \mu, \phi) \\ &= \int_0^{2\pi} \int_{-1}^1 \mathbf{S}(\mu, \phi, \mu', \phi') \mathbf{I}_d(\omega, \tau, \mu', \phi') d\mu' d\phi' \\ &+ \mathbf{F}_o(\mu, \phi) f(\omega, \tau) \exp(-\tau), \text{ for } 0 \leq \tau \leq \tau_o \end{aligned} \quad (12)$$

where  $\mathbf{F}_o = \mathbf{S}(\mu, \phi, 1, 0) \mathbf{I}_o$ , and  $f(\omega, \tau)$  is the Fourier transform of  $f(t, \tau)$  given by

$$f(\omega, \tau) = \exp\left(-i\omega \frac{\tau}{\tau_o}\right) 2\pi \delta(\omega - \omega_m). \quad (13)$$

Using  $\omega = \omega_m + \omega'$  and  $\mathbf{I}'_d(\omega, \tau) = \mathbf{I}_d \exp(-i\omega\tau/\tau_o)$ , Eq. (12) is transformed to

$$\begin{aligned} & \left[\mu \frac{\partial}{\partial \tau} + 1 + (\mu - 1) i \frac{\omega' + \omega_m}{\tau_o}\right] \mathbf{I}'_d(\omega', \tau, \mu, \phi) \\ &= \int_0^{2\pi} \int_{-1}^1 \mathbf{S}(\mu, \phi, \mu', \phi') \mathbf{I}'_d(\omega', \tau, \mu', \phi') d\mu' d\phi' \\ &+ \mathbf{F}_o(\mu, \phi) f(\omega', \tau) \exp(-\tau), \text{ for } 0 \leq \tau \leq \tau_o \end{aligned} \quad (14)$$

where

$$f(\omega, \tau) = 2\pi \delta(\omega'). \quad (15)$$

Equation (14) is solved by using boundary conditions

$$\mathbf{I}'_d(\tau = 0) = 0 \quad \text{for } 0 \leq \mu \leq 1 \quad (16)$$

$$\mathbf{I}'_d(\tau = \tau_o) = 0 \quad \text{for } -1 \leq \mu \leq 0. \quad (17)$$

The solution from Eq. (14) is in the frequency domain. To transform into the time domain, we use

$$\mathbf{I}_d(t, \tau) = \frac{1}{2\pi} \int \mathbf{I}'_d(\omega', \tau) \exp\left(i\omega \frac{\tau}{\tau_o} - i\omega' t\right) d\omega'. \quad (18)$$

We can further reduce the variable under assumption that the azimuthal domain is symmetrical due to the plane parallel geometry. The azimuthal dependence can be expanded using Fourier series

$$\begin{aligned} \mathbf{I}'_d(\tau, \mu, \phi, t) &= \mathbf{I}'_d^{(0)}(\tau, \mu, t) \\ &+ \sum_{n=1}^{\infty} \left[ \mathbf{I}'_{dc}^{(n)}(\tau, \mu, t) \cos(n\phi) + \mathbf{I}'_{ds}^{(n)}(\tau, \mu, t) \sin(n\phi) \right]. \end{aligned} \quad (19)$$

For linear polarization, there are only two non-zero modes in mode 0 ( $n = 0$ ) and mode 2 ( $n = 2$ ). On the other hand, for circular polarization, only mode zero is non-zero. Therefore, we can write Eq. (14) with the reduction of the  $\phi$  variable as

$$\begin{aligned} & \mu \frac{\partial}{\partial \tau} \mathbf{I}'_d(\omega', \tau, \mu) + \left[ 1 + (\mu - 1) i \frac{\omega' + \omega_m}{\tau_o} \right] \mathbf{I}'_d(\omega, \tau, \mu) \\ &= \int_{-1}^1 \mathbf{L}(\mu, \mu') \mathbf{I}'_d(\omega', \tau, \mu') d\mu' \\ &+ \mathbf{F}_o(\mu) f(\omega', \tau) \exp(-\tau), \text{ for } 0 \leq \tau \leq \tau_o \end{aligned} \quad (20)$$

where  $\mathbf{L}$  is

$$\mathbf{L}(\mu, \mu') = \int_0^{2\pi} \mathbf{S}(\mu, \mu', \phi' - \phi) d(\phi' - \phi). \quad (21)$$

The solution of Eq. (20) can be computed numerically. With the use of the Gauss quadrature, we approximate the integration as a summation of  $2N$  terms ( $-N \dots -1, 1, \dots, N$ ) [6]. Then, Eq. (20) become a matrix equation. Note that this number of Gauss quadrature affects the computational time tremendously. In our calculations, we use  $N = 40$ . The solution to the matrix equation leads to the solution of the diffuse component of the modified Stokes vector. The solution for the coherent component of the modified Stokes vector is given in Eq. (10). Thus, by combining these two solutions, we can reconstruct the optical signal propagating through a random scattering medium. In all our results, we use the vertically linear polarization where

$$\mathbf{I}_o = [1 \quad 0 \quad 0 \quad 0]^T. \quad (22)$$

#### 4. Results and Discussions

In general, the scattering random medium induces absorption and scattering in the input signal. Therefore, there are two main considerations to the characterization of the channel. First, the loss due to the absorption which causes the reduction of the signal-to-noise ratio. The solution to this problem is either increasing the transmission power, gain of the receiver, or changing the wavelength of the carrier optical frequency to reduce the loss. There are certain limitations to these solutions. The transmission power is limited

to a certain regulated amount because of the safety concern, while the change of wavelength is limited by the available frequency range. Thus, the attenuation is considered in our calculation but will not be the main focus here. The other degradation of the signal is the signal waveform distortion created by the scattering effect. In the view of communication theory, the random medium can be realized as a transfer function in the frequency domain or an impulse response in the time domain. The random medium acts like a low-pass filter. Due to the band limited nature of the medium, the signal will suffer from spreading and Inter Symbol Interference (ISI). Our results and discussions will concentrate on characterization of this signal distortion effect according to the medium when properties of medium, input signal, and receiver vary.

#### 4.1 FSO Characteristics

First, we consider the frequency response of the channel. The randomness of the channel is governed by the optical depth ( $\tau_o$ ) value; thus, we plot the frequency response when optical depth varies in Fig. 4. The results show that the channel acts as a low-pass filter. The greater the optical depth, the more pronounced the low-pass effect. The channel also shows a non-linear phase response which indicates signifi-

cant distortion.

Figure 5 shows the AC component wave form of the output signal at the modulation frequency of 50 MHz corresponding to a 100 Mbit per second data transmission. Since we only combine the contribution of the wave up to the ninth harmonic, even when a signal encounter small randomness (optical depth of 1) it is not a perfectly square wave. Each frequency component encounters different attenuation and phase shift (or time delay). Therefore, at the receiver, the composition of the wave shows signs of distortion. The more randomness the signal encounters, i.e. the larger the optical depth, the more distorted the signal output becomes as shown in Fig. 5(b).

Since the distorted portion of the signal is the result of the diffuse component, the larger the diffuse component, the larger the distortion. Here, the coherent component is attenuated at the rate of  $\exp(-\tau_o)$ , while the diffuse component increase as  $\tau_o$  gets larger. Therefore, we can roughly classified the behavior of the signal into two categories: the coherent dominate regime and the incoherent dominate regime. In the coherent dominate regime, the signal distortion is minimal because signal does not endure the scattering effect. However, the signals show considerable distortion in the incoherent dominate regime. The FOV of the receiver also

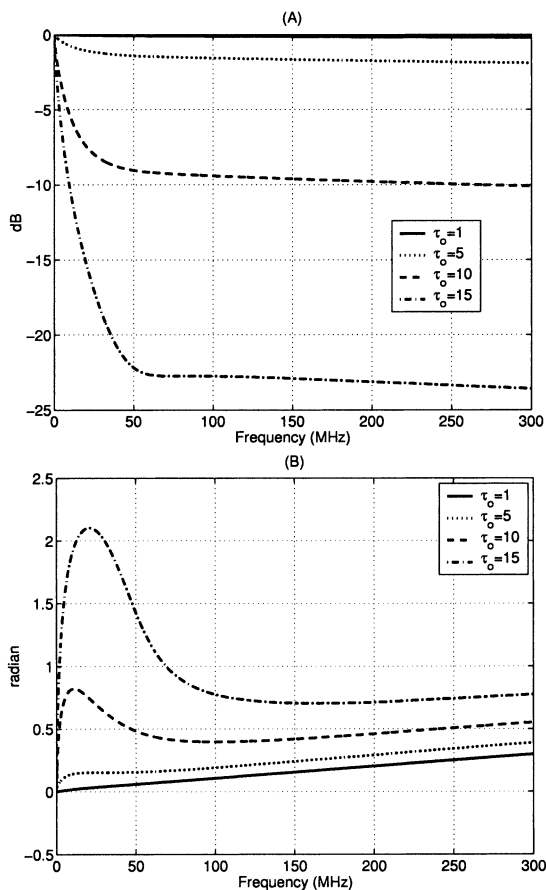


Fig. 4 Frequency response of an FSO channel (A) Magnitude (dB) and (B) Phase.

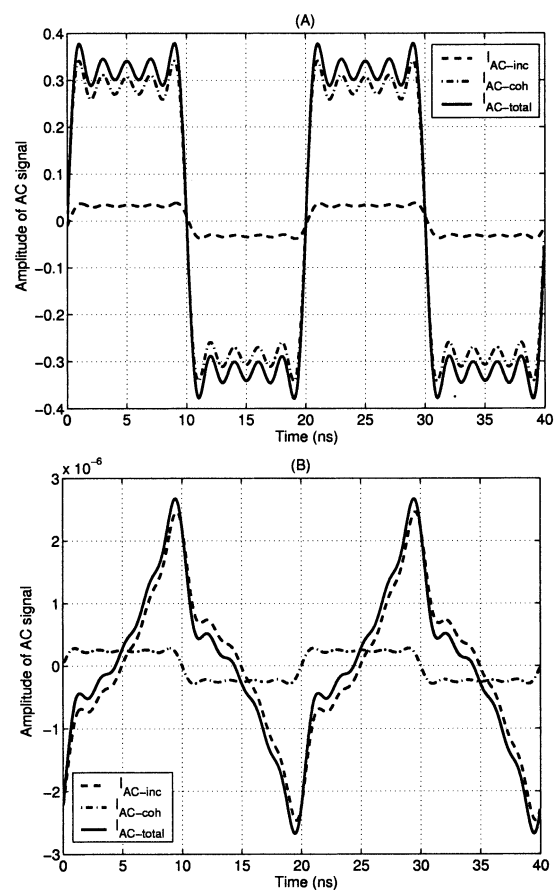


Fig. 5 Received ac signal at the receiver with FOV of 50 mrad at 50 MHz modulation (A)  $\tau_o = 1$  and (B)  $\tau_o = 15$ .

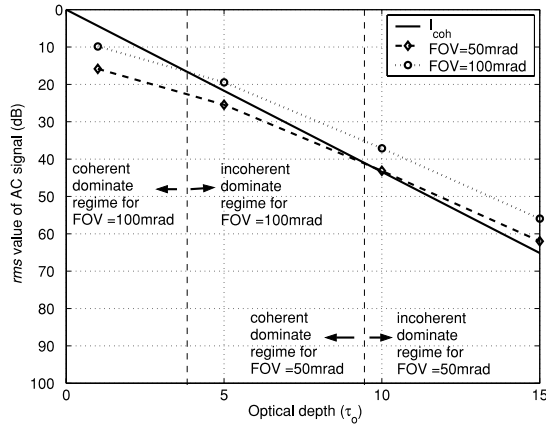


Fig. 6 Comparison of rms value of incoherent and coherent components as a function of optical depth at 50 MHz modulation when FOV varies.

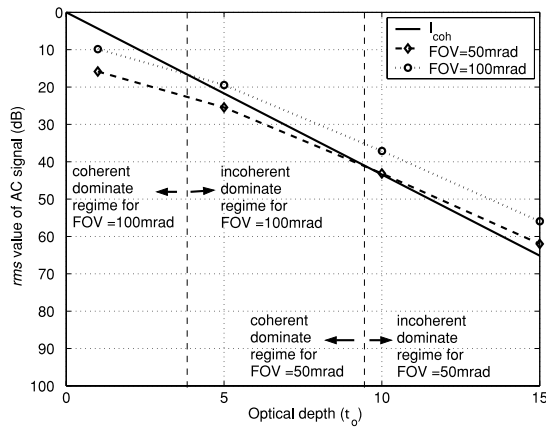


Fig. 7 Comparison of rms value of incoherent and coherent components as a function of optical depth at 500 MHz modulation when FOV varies.

has a strong effect on the distortion of the signal because it dictates the amount of diffuse component received. The obvious question might be why not let the FOV be very small so that we limit the distorted signal. The answer is that the reduction of the FOV is limited by the physical receiver dimension. More importantly, when the optical depth gets larger, the coherent component becomes so small that we cannot detect anything. The incoherent component may be used in those cases. Figure 6 shows where the coherent and incoherent dominate regimes lie as a function of optical depth in our numerical examples. Notice that when the FOV increases, the intersection point of coherent and incoherent components shifts to the left indicating that the incoherent dominated region occurs at a smaller value of optical depth.

The choice of modulation frequency, which infers the bit rate, is also very important. Figure 7 shows the coherent and incoherence dominate regions in the case of a 500 MHz modulation frequency. When compared with the 50 MHz modulation frequency shown in Fig. 6, the incoherent dominate region shifts to larger optical depth value when the modulation frequency increases.

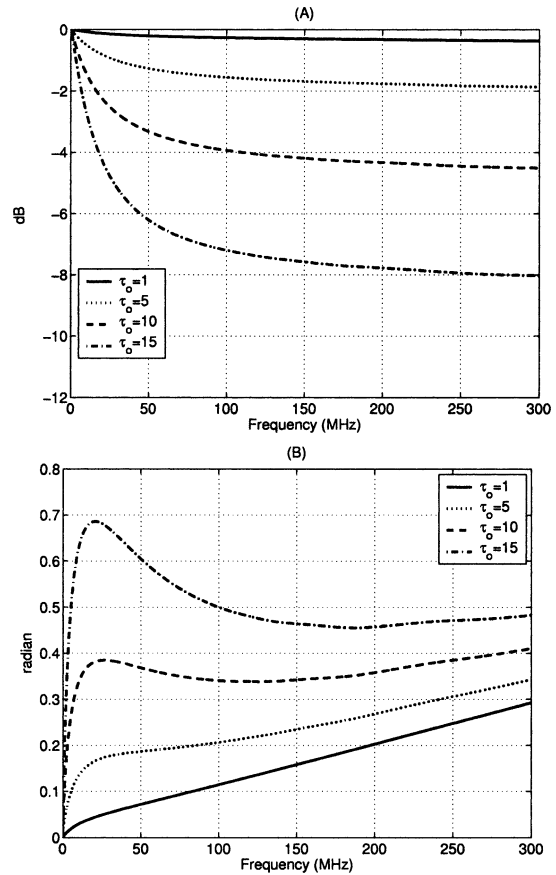


Fig. 8 Frequency response of an MMW channel with rain rate of 100 mm/hr (A) Magnitude (dB) and (B) Phase.

#### 4.2 Millimeter Wave Communication Characteristics

We show the frequency response of the MMW channel as a function of the optical depth in Fig. 8. The results show the low-pass behavior and non-linear phase response, but both are weaker when compared to FSO channel. It indicates that MMW communication suffers less ISI effect from multiple scattering.

Figure 9 shows the AC component wave form of the output signal at the modulation frequency of 50 MHz, which can be compared to Fig. 5 in FSO case. Only difference here is the FOV which is larger in this case. Even with larger FOV which include more scattering effects, the signals show less distortion than those in FSO case. This conclusion corresponds to the frequency response characteristics stated previously.

We compare the effect of rain rate in Fig. 10. The results show that the higher the rain rate, the more the scattering effect because when the rain rate is high, the incoherent dominate regime occurs when optical depth is small. This can be explained by the fact that at higher rain rate, the average size of particles are larger, which results in more forward scattering.

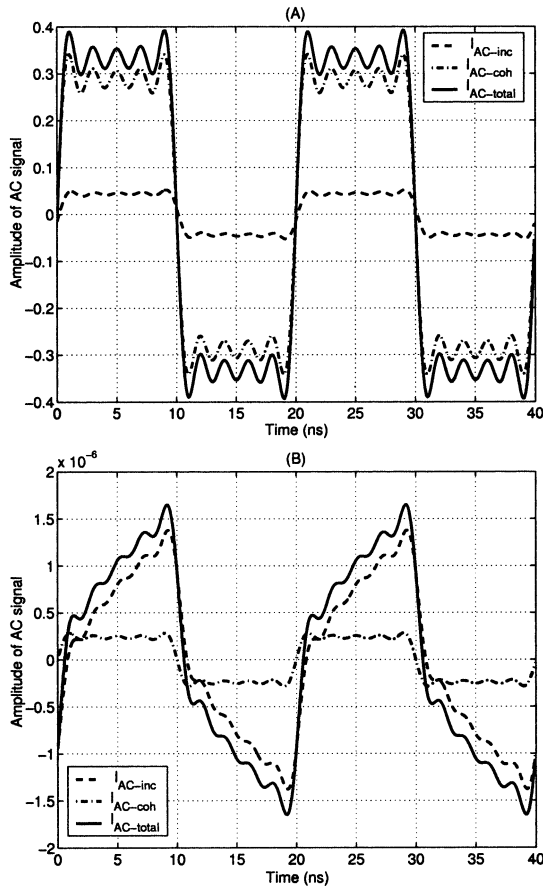


Fig. 9 Received ac signal at the receiver with FOV of 200 mrad at 50 MHz modulation for rain rate of 100 mm/hr (A)  $\tau_o = 1$  and (B)  $\tau_o = 15$ .

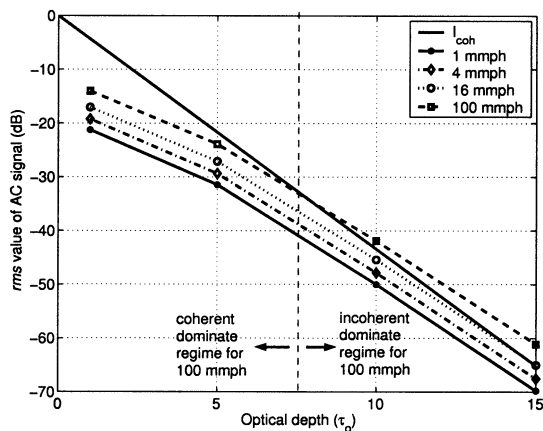


Fig. 10 Comparison of rms value of incoherent and coherent components as a function of optical depth at 50 MHz modulation when rain rate varies.

5. Conclusions

We explain the use of radiative transfer theory for the point-to-point wireless channel characterization including the justifications and limitations. We express the formulation and solution of the frequency-dependent vector-radiative trans-

fer equation. Based on these solutions, we are able to study several aspects of the channel characterization, including the properties of random medium, input signal and receivers. From the numerical calculations, we show that the distortion of the signal waveform occurs when the signal propagates through a random scattering medium, especially in the incoherent dominated regime. Both optical wave and MMW are investigated. We show the effect of the FOV of the receiver which dictates the domination of the coherent and incoherent components. This is useful information indicating where communication is feasible.

Acknowledgments

This work has been supported by Terabeam Corporation and NSF (ECS-9908849).

References

- [1] H.C. van de Hulst, Multiple Light Scattering, Academic, New York, 1980.
- [2] S. Jaruwatanadilok, A. Ishimaru, and Y. Kuga, "Photon density wave for imaging through random media," Wave in Random Media, vol.12, pp.351-364, 2002.
- [3] U. Ketprom, Y. Kuga, S. Jaruwatanadilok, and A. Ishimaru, "Numerical studies on time-domain responses of on-off-keyed modulated optical signals through a dense fog," Appl. Opt., vol.43, no.2, pp.496-505, 2004.
- [4] B.J. Tromberg, L.O. Svaasand, T.-T. Tsay, and R.C. Haskell, "Properties of photon density waves in multiple scattering media," Appl. Opt., vol.32, pp.607-616, 1993.
- [5] J.B. Fiskin, S. Fantini, M.J.V. Ven, and E. Gratton, "Gigahertz photon density waves in a turbid medium: Theory and experiments," Phys. Rev. E, vol.53, pp.2307-2319, 1996.
- [6] A. Ishimaru, Wave Propagation and Scattering in Random Media, IEEE Press, New York, 1997.
- [7] NIRE, "Measurement of size distribution of aerosol by bistatic system," <http://www.aist.go.jp/NIRE/annual/1999/21.htm>, 2000.
- [8] D. Kedar and S. Arnon, "Optical wireless communication through fog in the presence of pointing error," Appl. Opt., vol.42, pp.4946-4954, 2003.
- [9] J.S. Marshall and W. McK. Palmer, "The distribution of raindrops with size," J. Meteorology, vol.5, pp.165-166, 1948.
- [10] A. Ishimaru, S. Jaruwatanadilok, and Y. Kuga, "Polarized pulse waves in random discrete scatterers," Appl. Opt., vol.40, pp.5495-5502, 2001.
- [11] R.M. Gagliardi and S. Karp, Optical Communications, John Wiley & Sons, New York, 1995.
- [12] R.L. Cheung and A. Ishimaru, "Transmission, backscattering and depolarization of waves in randomly distributed spherical particles," Appl. Opt., vol.21, pp.3792-3798, 1982.



**Serm Sak Jaruwatanadilok** was born in Bangkok, Thailand. He received his B.E. degree from King Mongkut's Institute of Technology, Ladkrabang, Thailand in 1994, M.S. degree from Texas A&M University, College Station, Texas, USA in 1997, and Ph.D. degree from University of Washington, Seattle, USA in 2003. He is now a research associate at the University of Washington, Seattle. His research interest lies in the area of remote sensing and waves in random media.



**Urachada Ketprom** was born in Bangkok, Thailand. She received her BSEE from Northwestern University, Evanston, Illinois in 1997 and MSEE from the University of Washington, Seattle, Washington in 1999. In the present, she is pursuing her Ph.D. degree at the University of Washington. Her current research involves numerical and experimental studies of optical wave propagation through random media.



**Yasuo Kuga** was born in Kitakyushu, Japan. He received his B.S., M.S., and Ph.D. degrees from the University of Washington, Seattle, USA in 1977, 1979, and 1983, respectively. He is currently a Professor of electrical engineering at the University of Washington. From 1983 to 1988, he was a Research Assistant Professor of electrical engineering at the University of Washington. From 1988 to 1991, he was an Assistant Professor of electrical engineering and computer science at the University of Michigan,

Ann Arbor. Since 1991, he has been with the University of Washington. He was an Associate Editor of *Radio Science* (1993–1996) and *IEEE Trans. Geoscience and Remote Sensing* (1996–2000). He was elected to IEEE Fellow in 2004. He was also elected as a 1989 Presidential Young Investigator. His research interests are in the areas of microwave and millimeter-wave remote sensing, high-frequency devices, and optics.



**Akira Ishimaru** received the B.S. degree in 1951 from the University of Tokyo, Tokyo, Japan, and the Ph.D. degree in electrical engineering in 1958 from the University of Washington, Seattle. From 1951 to 1952, he was with the Electrotechnical Laboratory, Tanashi, Tokyo, and in 1956, he was with Bell Laboratories, Holmdel, NJ. In 1958, he joined the faculty of the Department of Electrical Engineering of the University of Washington, where he was a Professor of electrical engineering and an Adjunct Professor of applied mathematics. He is currently Professor Emeritus there. He has also been a Visiting Associate Professor at the University of California, Berkeley. His current research includes waves in random media, remote sensing, object detection, and imaging in clutter environment, inverse problems, millimeter wave, optical propagation and scattering in the atmosphere and the terrain, rough surface scattering, and optical diffusion in tissues. He is the author of *Wave Propagation and Scattering in Random Media* (New York: Academic, 1978; IEEE-Oxford University Press Classic reissue, 1997) and *Electromagnetic Wave Propagation, Radiation, and Scattering* (EnglewoodCliffs, NJ: Prentice-Hall, 1991). He was Editor (1979–1983) of *Radio Science* and Founding Editor of *Waves in Random Media*, Institute of Physics, U.K. Dr. Ishimaru has served as a member-at-large of the U.S. National Committee (USNC) and was chairman (1985–1987) of Commission B of the USNC/International Union of Radio Science. He is a Fellow of the Optical Society of America, the IEEE, the Acoustical Society of America, and the Institute of Physics, U.K. He was the recipient of the 1968 IEEE Region VI Achievement Award and the IEEE Centennial Medal in 1984. He was appointed as Boeing Martin Professor in the College of Engineering in 1993. In 1995, he was awarded the Distinguished Achievement Award from the IEEE Antennas and Propagation Society. He was elected to the National Academy of Engineering in 1996. In 1998, he was awarded the Distinguished Achievement Award from the IEEE Geoscience and Remote Sensing Society. He is the recipient of the 1999 IEEE Heinrich Hertz Medal and the 1999 URSI Dellinger Gold Medal. In 2000, he received the IEEE Third Millennium Medal.